Journal of Manufacturing Processes
Vol. 6/No. 1
2004

Technical Note

A Multiscale Fabrication Approach to Microfluidic System Development

T.L. Schmitz, Dept. of Mechanical and Aerospace Engineering, University of Florida, Gainesville, Florida, USA
J.A. Dagata and **B. Dutterer,** National Institute of Standards and Technology, Gaithersburg, Maryland, USA
W. Gregory Sawyer, Dept. of Mechanical and Aerospace Engineering, University of Florida, Gainesville, Florida, USA

Abstract

Microfluidic systems for analytical, medical, and sensing applications integrate optical or electrical readouts in low-cost, low-volume consumption systems. Embedding chemically functionalized templates with nanoscale topography within these devices links the scale at which molecular recognition/self-organization occurs and the macroscopic layout of fluid channels, mixing volumes, and detection regions. Although the design of a platform that would meet the needs of all microfluidic experiments is a difficult undertaking, this paper provides a description of a flexure-based platform that may address generic requirements such as low cost, ease of manufacture, and repeatable alignment/sealing performance. Experimental results are provided for master replication in plastics by hot embossing and a microfluidic platform that orients 125 micrometer channels embossed in a poly(vinyl chloride) gasket to an array of high-speed machined channels.

Keywords: *Flexure, Hot Embossing, High-Speed Machining*

Introduction

The use of microfluidic systems in biological, analytical, medical, and sensing applications is continually growing. Applications include, for example, DNA and protein analysis and studies of synergistic/antagonistic interactions between multiple drug substances (high-throughput drug screening, or HTS). To date, many research efforts have focused on the ability to either produce sub-micrometer-scale features on substrates, such as silicon, or replicate these substrate features in polymers [e.g., 1-30]. However, less attention has been given to the overall manufacturing perspective, including the required infrastructure for low to high-volume production of microfluidic testing components. This paper describes initial efforts in the development of a suite of manufacturing procedures for the production and rapid replication of microfluidic testing hardware, including the master substrate with desired features and the experimental platform. Although it is a challenging task to design a platform that would meet the needs of all microfluidic experiments, a description is presented here of a flexure-based platform that may address generic requirements such as low cost, ease of manufacture, and repeatable alignment/sealing performance. These benefits could, in turn, lead to improved laboratory efficiency, decreased development time, and more convenient sharing of results between multiple laboratories. The manufacturing methods described include: (1) scanning probe lithography to produce sub-50 nanometer-scale features on a standard-sized silicon master; (2) hot embossing for polymer replication of the nanometer-scale silicon master and/or the production of larger-scale features (=100 μm) used to connect the macroscale fluid input ports to the nanometer-scale patterns under test; and (3) high-speed machining for the production of the microfluidic experimental platform, as well as any hot embossing tooling required for larger-scale features.

Manufacturing Methods

This section presents an overview of the production methods applied in this research (note that this list is not comprehensive; other fabrication processes are also available). Using these methods, it is possible to span several orders of magnitude, for ex-

ample, nanometer to centimeter, in the characteristic length of the manufactured feature or part.

Scanning Probe Lithography

In scanning probe lithography (SPL), an electrical bias is applied between the silicon substrate and an atomic force microscope (AFM) cantilever tip [31-32]. In the presence of water (as vapor in the air or condensation on the silicon surface), an electrochemical cell is formed in which the AFM tip serves as the cathode, the silicon substrate as the anode, and the liquid column as a 'dielectric bridge,' as shown in *Figure 1*. Anodic oxidation proceeds as the silicon gives up electrons to become positively charged and these electrons serve to reduce gaseous oxygen in the presence of water to form oxyanions (OH–). The combination of the silicon cations, gaseous oxygen, and water yields silicon dioxide and hydrogen anions. By translating the AFM tip relative to the silicon surface, nanometer-scale oxide patterns can be formed on the surface of the substrate. SPL therefore serves as a direct-writing and resistless prototyping method for nanometer-scale devices [33-34]. An example of features that can be produced using SPL is shown in *Figure 2* [31]. This figure shows scanning electron microscope (SEM) measurement results for oxide lines on a silicon wafer. The lines are approximately 40 nm wide and 100 nm high with lengths of 3 μm, 5 μm, and 10 μm. The pitch of the lines varies from 100 nm to 500 nm.

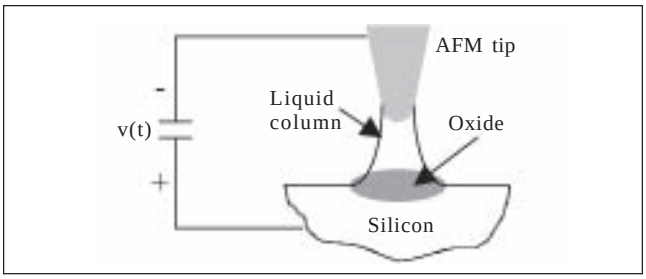

Figure 1
Schematic of Scanning Probe Lithography (SPL) Nanocell

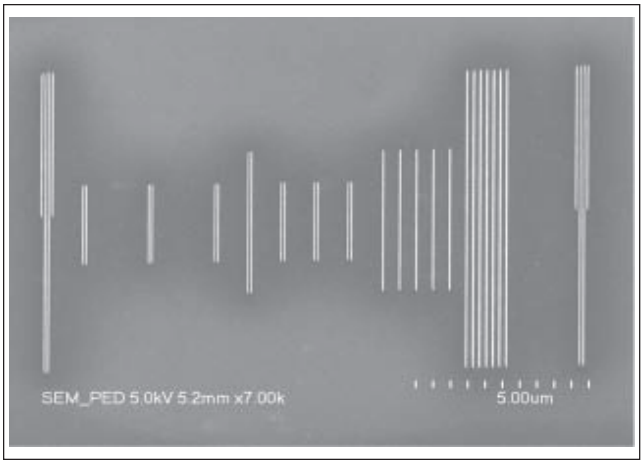

Figure 2
SEM Image of SPL Oxide Lines on Silicon Substrate [31]

Hot Embossing

Although SPL is useful for producing nanometer-scale devices, it is also a slow process. Therefore, efficient replication of the features produced on the silicon master in low-cost materials is necessary when completing multiple test cycles in a short period of time with one or more control variables in, for example, chemical analysis. Traditionally, the replication materials have been polymers (e.g., poly(dimethylsiloxane), or PDMS, and poly(methyl methacrylate), or PMMA) because they are generally inexpensive, mechanically robust, and optically transparent (to allow in-process viewing). Typical replication methods include casting, injection molding, and hot embossing [35]. This work focuses on hot embossing of poly(vinyl chloride), or PVC, and PMMA. In this technique, the polymer is first heated to its glass transition temperature, and then the desired features are forced into the plastic and held for a short time. Two experimental setups were used in this research. First, a vacuum hotplate was used to heat and hold PVC samples, while gravitational mass loading was employed to force the silicon substrate into the PVC. Second, a hydraulic press with a temperature-controlled base plate was used to force a silicon substrate into a PMMA sheet.

High-Speed Machining

Significant advancements in high-speed machining (HSM) technology, including new spindle designs for higher rotational speed, torque, and power, increased slide speeds and accelerations, new machine designs for lower moving mass, and tool material/coating developments, have made HSM a viable alternative to other manufacturing processes in many applications. For example, HSM has been used extensively in the aerospace industry, where the dramatic increases in material removal rates have allowed designers to replace assembly-intensive

sheet metal build-ups with monolithic aluminum components [36]. HSM has been applied in this research due to its inherent flexibility; it can produce features in a number of materials over the full size range required for this research (~100 μm to 10 cm, or roughly 3 orders of magnitude).

Flexure-Based Platform Development

The fundamental requirements identified for the microfluidic experimental platform included (1) the ability to align fluid inputs and outputs to a (patterned) gasket and silicon master or polymer reproduction; (2) optical transparency of the individual components for in-process evaluation; and (3) minimum manufacturing cost, time, and difficulty. *Figure 3* shows the concept for a prototype flexure-based platform that positions the inlet/outlet flow tubes, fixed with epoxy into holes drilled into the PMMA cover, relative to the base using a parallelogram leaf-type flexure arrangement. The flexure design was selected to allow repeatable sealing performance of the platform, as described in the next section. A patterned 1 cm × 2 cm PVC gasket is captured in a well-machined into the base. Although certainly not novel to this research study, flow visualization in the micrometer-scale channels was selected for initial testing of the platform performance. The 125 μm wide by 50 μm deep channels were high-speed machined (using a 125 μm diameter endmill) in the bottom of the well and no silicon master was used. In the following paragraphs, details of the prototype platform are described, including critical dimensions, flexure design, surface roughness measurements for machined surfaces, laminar flow characteristics, and preliminary hot embossing results.

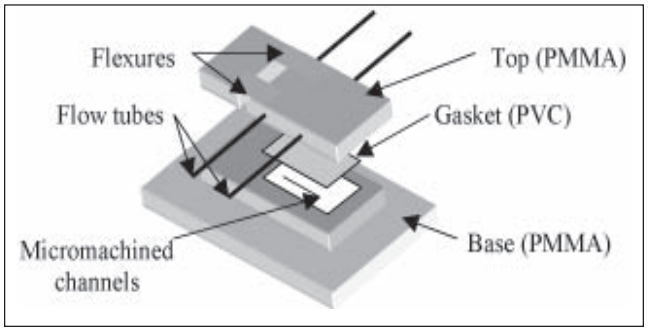

Figure 3
Flexure-Based Prototype Platform Schematic. The platform top is sealed against the gasket and channels through the nearly linear motion afforded by the flexures. Flow can then proceed through the flow tubes.

Flexure Design

The parallelogram leaf-type flexure design was selected to clamp the cover/gasket/base assembly due to its ability to provide repeatable, nearly linear motion and its ease of manufacture. The flexure dimensions are shown in *Figure 4*. A zero-slope condition at the free end of the flexure was obtained by applying the actuation force at a distance of one-half the flexure length from the fixed end. A depiction of the flexure motion under actuation is shown in *Figure 5*. When no actuation force is applied to the flexure top, the assembly is open and the gasket is not sealed against the silicon master. However, under the actuation force, the gasket is sealed against the master and fluid flow can proceed. Once the force is removed, the flexure top returns to its original (open) position. Following the analysis of Smith [37], the minimum leaf flexure length to avoid plastic deformation, L_{min}, parasitic deflection, δ_x, and actuation force, F_y, were calculated according to Eqs. (1)-(3), where E is the PMMA modulus (3×10^9 Pa), Y is the yield strength (6.7×10^7 Pa), δ_y is the required deflection (0.5 mm), t is the leaf flexure thickness (0.4 mm), w is the total width of the two flexure arms (4.0 mm), and L is the length (7.5 mm). The predicted δ_x value was incorporated into the platform design to minimize positioning errors between the flow tubes and base.

$$L_{\min} = \left(\frac{3e\delta_y t}{Y} \right)^{\frac{1}{2}} = 5.2\,\text{mm} \tag{1}$$

$$\delta_x = \frac{-3\delta_y^{\,2}}{5L} = -0.02\,\text{mm} \tag{2}$$

$$F_y = \frac{wt^3 E\delta_y}{L^3} = 1\,\text{N} \tag{3}$$

Platform Surface Roughness Measurements

Once the platform cover and base (also PMMA) were machined, surface roughness measurements were performed using a scanning white light interferometer (5X objective, 1.2 mm × 1 mm field of view). Microscopic images of the 125 μm wide by 75 μm deep channels and 800 μm diameter by 200

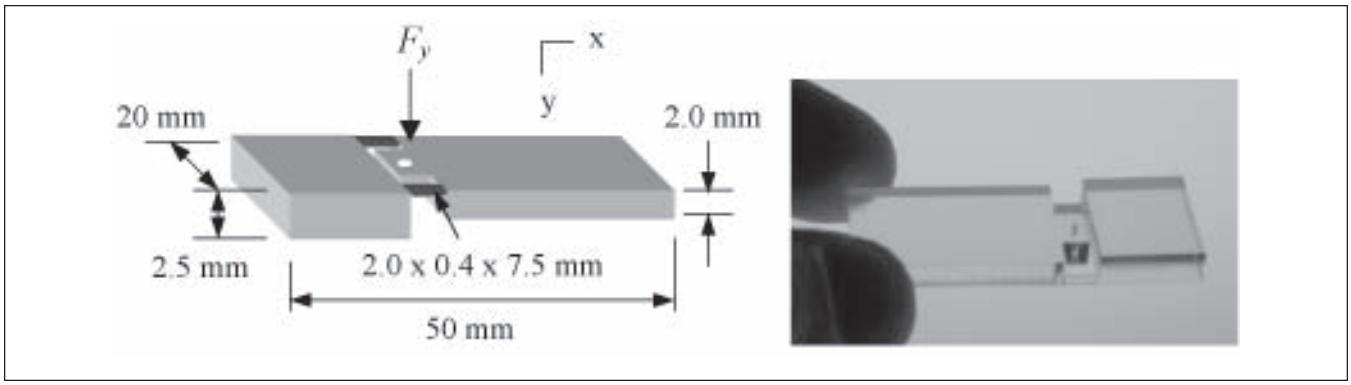

Figure 4
Flexure Dimensions and Photograph of Machined Component

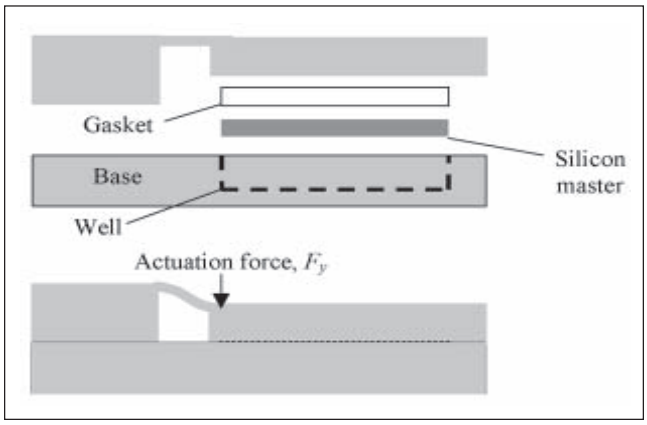

Figure 5
Schematic of Microfluidic Testing Platform Actuation

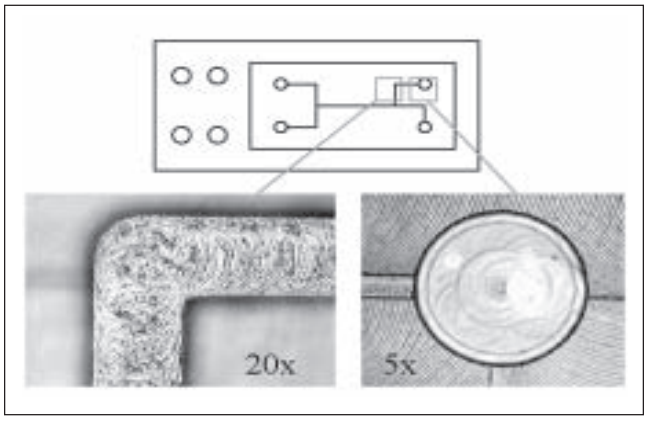

Figure 6
Microscope Images of Micromachined Channel and Hole. The channel is 125 µm wide; the hole has an 800 µm diameter.

µm deep holes machined into the well located in the base are shown in *Figure 6*. An example line-trace roughness measurement for a channel bottom is shown in *Figure 7* (the average roughness for the measured area was 0.31 µm).

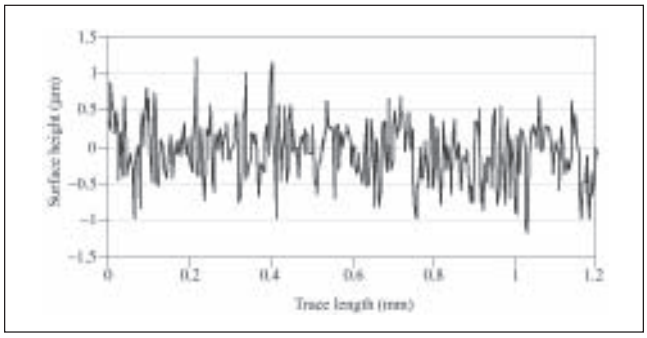

Figure 7
Channel Roughness Measurement

Laminar Flow Measurements

To verify the alignment, sealing, and flow performance of the prototype platform, the flow characteristics in the milled channels were observed. Water mixed with yellow (Y) and blue (B) dye was introduced to the assembled platform via the flow tubes, as shown schematically in *Figure 8* (other flow patterns were also evaluated). The 10X microscope images included in this figure show laminar behavior with very little boundary diffusional mixing over the short length scales of 12 mm or less used in this research (see the sharp corner at the top T-junction, for example). The low Reynolds numbers, and subsequent laminar flows, in typical microchannels can, in fact, be problematic in situations where mixing is required, such as the homogenization of reagents in chemical reactions [3]. An important area of future research for SPL is, therefore, the fabrication of structured features that lead to efficient mixing over short distances. However, in this case, it was desired to determine if the surface roughness introduced by the micromachining process would be low enough to allow laminar flow.

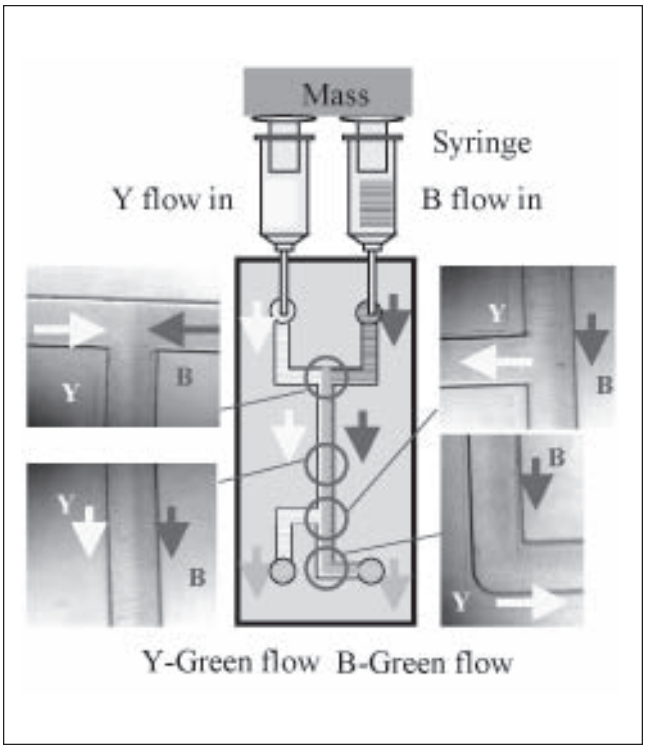

Figure 8
Laminar Flow Visualization in Micromachined Channels

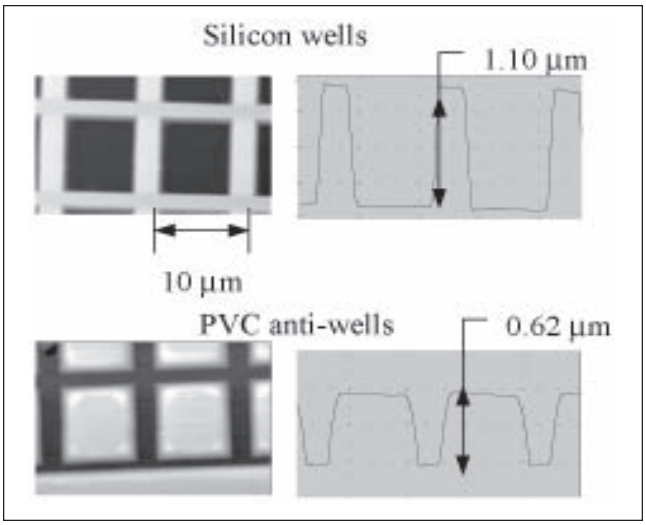

Figure 9
Hot Embossing Results for Silicon Wells Reproduced in 1 mm Thick PVC Sheet

Hot Embossing Results

PVC

Replication of micrometer-scale features in 1 mm thick PVC sheet by hot embossing from both silicon masters and larger machined tooling was completed. The flexible PVC sheet was selected due to its low modulus and ability to form a seal between the PMMA flexure cover and platform base. Macro pressures of 7×10^3 Pa to 14×10^3 Pa (localized pressures under the actual features were much higher, but unknown) were applied using a deadweight load at temperatures from 90°C to 160°C during the hot embossing. Microscope images (left) and AFM measurements (right) for 10 µm wide wells in a silicon master and corresponding anti-wells in PVC are shown in *Figure 9*. It can be seen that the lateral dimensions were accurately reproduced in the PVC, while the heights were not, that is, 1.10 µm silicon well depths versus 0.62 µm PVC anti-well heights. This is due to the viscoelastic behavior of the PVC.

Figure 10 shows microscope images and AFM measurements for silicon posts reproduced using the same hot embossing conditions. Again, it is seen that the heights were not reproduced with high fidelity, that is, 1.08 µm high silicon posts versus 0.74 µm deep PVC anti-posts. Additionally, there was substantial relaxation of the PVC within the embossed cavities so that the flat tops of the silicon posts were not accurately replicated.

To test the feasibility of combining hot embossed channels in PVC with high-speed machined channels in the platform base to achieve more complicated, multilevel flow patterns, a high-speed machined copper tool was used to emboss a PVC gasket with the geometry shown in *Figure 11*. The scanning white light interferometer measurements in this figure show the tool (80 µm high walls separated laterally by 1 mm) and embossed PVC (13 µm deep channels); the PVC relaxation at the larger scale is clearly quite severe. This patterned gasket was then sealed against the platform base and fluid flow was introduced (again using syringes as demonstrated in *Figure 8*) to the crossed pattern shown in *Figure 12*. In the left two microscope images, yellow fluid flow was coupled into both inputs and yellow fluid flow was observed at both outputs. In the right two images, yellow was input to the left-hand port and blue to the right-hand port. In this case, yellow flow was seen at the left-hand output and blue-green flow was observed from the right-hand output.

PMMA

In many instances, particularly testing scenarios with multiple input variables, it is desired to pro-

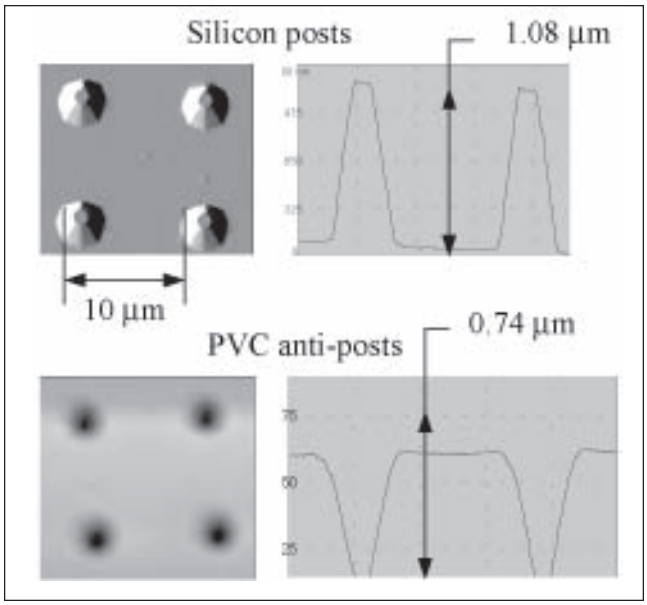

Figure 10
Hot Embossing Results for Silicon Posts Reproduced in 1 mm Thick PVC Sheet

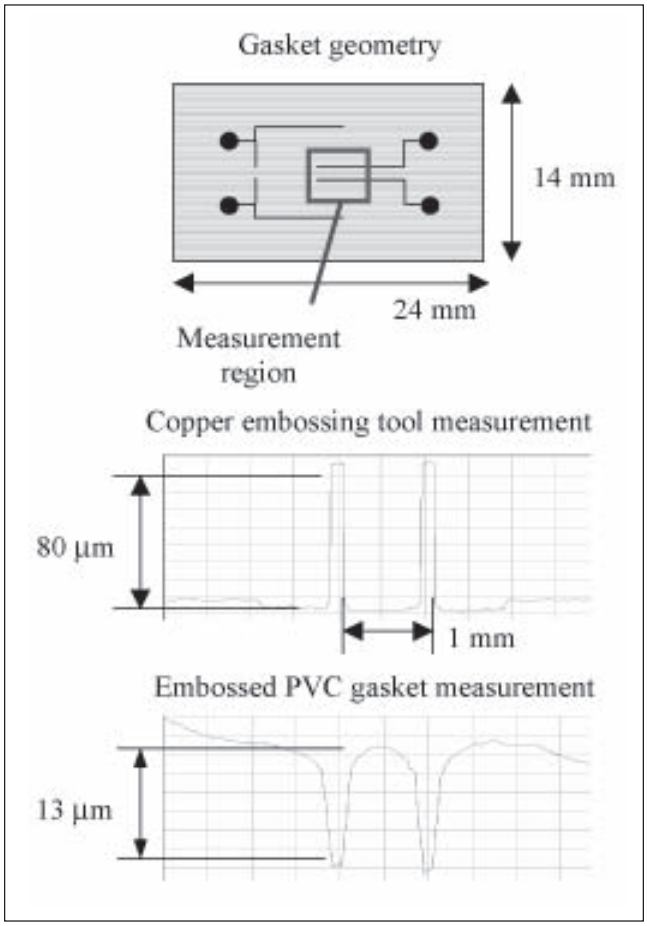

Figure 11
Measurement Results for Hot Embossing 1 mm Thick PVC Sheet Using High-Speed Machined Copper Tool

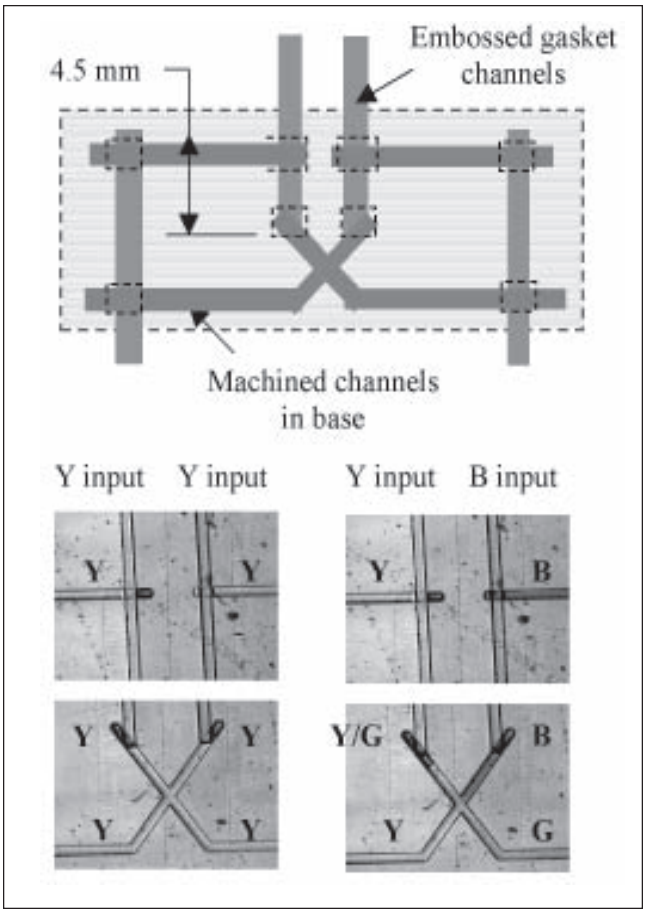

Figure 12
Flow Results for Hot Embossed Gasket/Micromachined Channels. Yellow and blue fluids were input using the scheme shown in *Figure 8*.

duce a single master substrate and then replicate the patterned surface in polymer many times to produce the microfluidic test components. Therefore, hot embossing was also carried out to transfer micrometer-scale features from a silicon master to 6.35 mm thick PMMA sheet. Scanning white light interferometer measurement results for the silicon master are shown in *Figure 13*. The raised squares are each approximately 1.04 µm tall and 30 µm wide. A two-dimensional cross section for one row of the repeated squares is shown in *Figure 14*. Embossing was carried out at approximately 120°C with low pressure (amplitude not recorded) applied for a few seconds before removing the PMMA sheet. An example measurement for the replicated features is shown in *Figure 15*. A two-dimensional cross section for one row of the repeated squares is shown in *Figure 16*. Good fidelity is observed for both the lateral spacing and feature depths. The improved replication accuracy

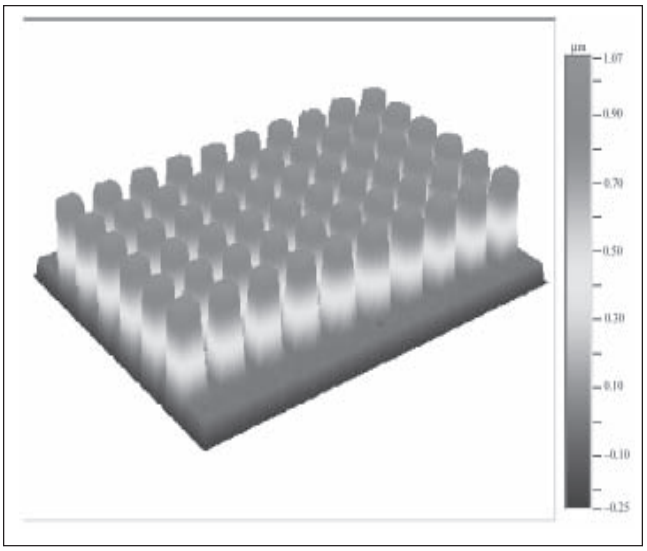

Figure 13
Silicon Master Measurement Result

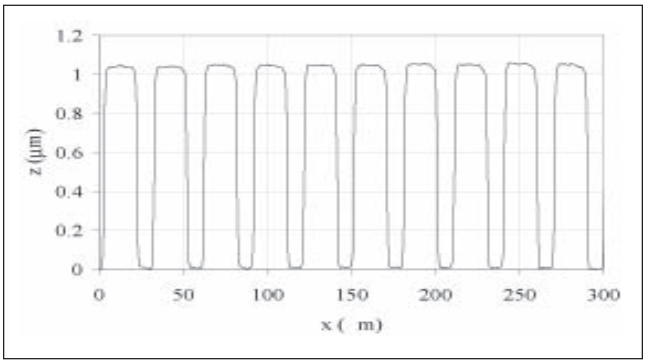

Figure 14
Two-Dimensional Cross Section for Silicon Master

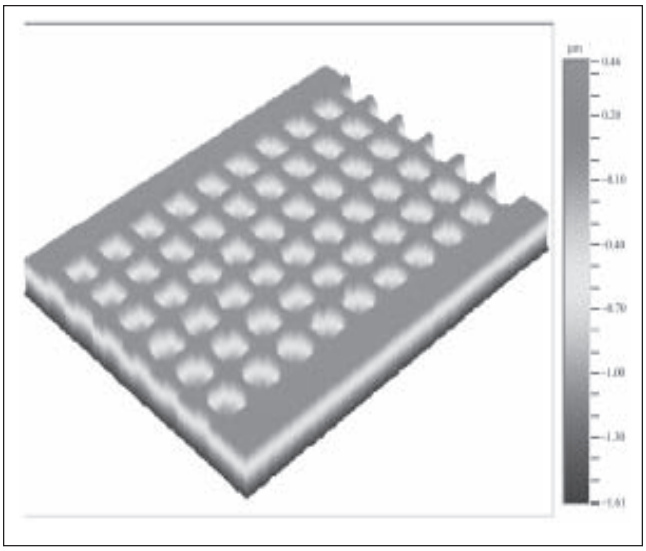

Figure 15
Hot Embossed Acrylic Sheet Measurement Result

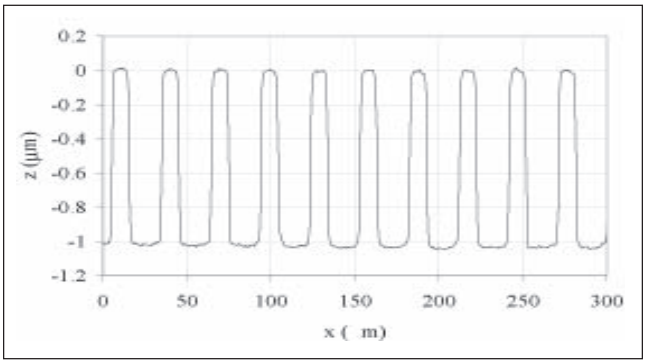

Figure 16
Two-Dimensional Cross Section for Hot Embossed Acrylic Sheet

of the PMMA over the PVC is a result of the lower viscoelastic recovery of the PMMA after removing the embossing pressure.

Summary

This paper described initial efforts toward the development of a suite of manufacturing methods for the production and rapid replication of a flexure-based microfluidic testing platform, designed to offer low cost, ease of manufacture, and repeatable alignment/sealing performance. Although considerations must be made for specific requirements in different test setups, it is our hope that the flexure concept can be included as a general architecture for microfluidic testing platforms. The prototype platform behavior was evaluated by observing the flow characteristics in high-speed machined 125 μm wide channels. Flow through a combination of embossed channels in a PVC gasket and machined channels in the platform base was also exhibited.

Acknowledgments

The authors acknowledge partial financial support for this research from the Manufacturing Metrology Division, National Institute of Standards and Technology, Gaithersburg, MD.

References

1. Dasgupta, P.; Surowiec, K.; and Berg, J. (2002). "Flow of multiple fluids in a small dimension." *Analytical Chemistry* (v74, n7), pp208A-213A.
2. McDonald, J.; Chabinyc, M.; Metallo, S.; Anderson, J.; Stroock, A.; and Whitesides, G. (2002). "Prototyping of microfluidic devices in poly(dimethylsiloxane) using solid-object printing." *Analytical Chemistry* (v74, n7), pp1537-1545.

3. Stroock, A.; Dertinger, S.; Ajdari, A.; Mezic, I.; Stone, H.; and Whitesides, G. (2002). "Chaotic mixer for microchannels." *Science* (v295), pp647-651.
4. Tamanaha, C.; Whitman, L.; and Colton, R. (2002). "Hybrid macro-micro fluidics system for a chip-based biosensor." *Journal of Micromechanics and Microengineering* (v12), ppN7-N17.
5. Lin, L.; Cheng, Y.T.; and Chiu, C.J. (1998). "Comparative study of hot embossed micro structures fabricated by laboratory and commercial environments." *Microsystem Technologies* (v4), pp113-116.
6. Tan, H.; Gilbertson, A.; and Chou, S. (1998). "Roller nanoimprint lithography." *Journal of Vacuum Science and Technology B* (v16, n6), pp3926-3928.
7. Stix, G. (2002). "Soft manufacturing." *Scientific American* (v287, n2), pp30-31.
8. Juang, Y.J.; Lee, L.J.; and Koelling, K.W. (2002). "Hot embossing in microfabrication. Part I: Experimental, Part II: Rheological characterization and process analysis." *Polymer Engg. and Science* (v42, n3), pp539-566.
9. Shen, X.J.; Pan, L.W.; and Lin, L.W. (2002). "Microplastic embossing process: experimental and theoretical characterizations." *Sensors and Actuators A-Physical* (v97-8), pp428-433.
10. Scheer, H.C. and Schulz, H. (2001). "A contribution to the flow behaviour of thin polymer films during hot embossing lithography." *Microelectronic Engg.* (v56, n3-4), pp311-332.
11. Lee, G.B.; Chen, S.H.; Huang, G.R.; Sung, W.C.; and Lin, Y.H. (2001). "Microfabricated plastic chips by hot embossing methods and their applications for DNA separation and detection." *Sensors and Actuators B-Chemical* (v75, n1-2), pp142-148.
12. Heyderman, L.J.; Schift, H.; David, C.; Gobrecht, J.; and Schweizer, T. (2000). "Flow behaviour of thin polymer films used for hot embossing lithography." *Microelectronic Engg.* (v54, n3-4), pp229-245.
13. Schift, H.; David, C.; Gobrecht, J.; D'Amore, A.; Simoneta, D.; Kaiser, W.; and Gabriel, M. (2000). "Quantitative analysis of the molding of nanostructures." *Journal of Vacuum Science & Technology B* (v18, n6), pp3564-3568.
14. Schift, H.; Heyderman, L.J.; and Gobrecht, J. (2002). "Efficient replication of nanostructured surfaces." *Chimia* (v56, n10), pp543-546.
15. Russo, A.P.; Apoga, D.; Dowell, N.; Shain, W.; Turner, A.M.P.; Craighead, H.G.; Hoch, H.C.; and Turner, J.N. (2002). "Microfabricated plastic devices from silicon using soft intermediates." *Biomedical Microdevices* (v4, n4), pp277-283.
16. Qi, S.Z.; Liu, X.Z.; Ford, S.; Barrows, J.; Thomas, G.; Kelly, K.; McCandless, A.; Lian, K.; Goettert, J.; and Soper, S.A. (2002). "Microfluidic devices fabricated in poly(methyl methacrylate) using hot-embossing with integrated sampling capillary and fiber optics for fluorescence detection." *Lab on a Chip* (v2, n2), pp88-95.
17. Kricka, L.J.; Fortina, P.; Panaro, N.J.; Wilding, P.; Alonso-Amigo, G.; and Becker, H. (2002). "Fabrication of plastic microchips by hot embossing." *Lab on a Chip* (v2, n1), pp1-4.
18. Roos, N.; Schulz, H.; Bendfeldt, L.; Fink, M.; Pfeiffer, K.; and Scheer, H.C. (2002). "First and second generation purely thermoset stamps for hot embossing." *Microelectronic Engg.* (v61, n2), pp399-405.
19. Schift, H.; Heyderman, L.J.; Padeste, C.; and Gobrecht, J. (2002). "Chemical nano-patterning using hot embossing lithography." *Microelectronic Engg.* (v61, n2), pp423-428.
20. Rotting, O.; Ropke, W.; Becker, H.; and Gartner, C. (2002). "Polymer microfabrication technologies." *Microsystem Technologies* (v8, n1), pp32-36.
21. Heyderman, L.J.; Schift, H.; David, C.; Ketterer, B.; Auf der Maur, M.; and Gobrecht, J. (2001). "Nanofabrication using hot embossing lithography and electroforming." *Microelectronic Engg.* (v57, n8), pp375-380.
22. Schift, H.; David, C.; Gabriel, M.; Gobrecht, J.; Heyderman, L.J.; Kaiser, W.; Koppel, S.; and Scandella, L. (2000). "Nanoreplication in polymers using hot embossing and injection molding." *Microelectronic Engg.* (v53, n1-4), pp171-174.
23. Becker, H. and Heim, U. (2000). "Hot embossing as a method for the fabrication of polymer high aspect ratio structures." *Sensors and Actuators A-Physical* (v83, n1-3), pp130-135.
24. Becker, H. and Gartner, C. (2000). "Polymer microfabrication methods for microfluidic analytical applications." *Electrophoresis* (v21, n1), pp12-26.
25. Becker, H. and Heim, U. (1999). "Polymer hot embossing with silicon master structures." *Sensors and Materials* (v11, n5), pp297-304.
26. Schift, H.; Jaszewski, R.W.; David, C.; and Gobrecht, J. (1999). "Nanostructuring of polymers and fabrication of interdigitated electrodes by hot embossing lithography." *Microelectronic Engg.* (v46, n1-4), pp121-124.
27. Heckele, M.; Bacher, W.; and Muller, K.D. (1998). "Hot embossing - the molding technique for plastic microstructures." *Microsystem Technologies* (v4, n3), pp122-124.
28. Jaszewski, R.W.; Schift, H.; Gobrecht, J.; and Smith, P. (1998). "Hot embossing in polymers as a direct way to pattern resist." *Microelectronic Engg.* (v42), pp575-578.
29. Gerlach, A.; Knebel, G.; Guber, A.E.; Heckele, M.; Herrmann, D.; Muslija, A.; and Schaller, T. (2002). "High-density plastic microfluidic platforms for capillary electrophoresis separation and high-throughput screening." *Sensors and Materials* (v14, n3), pp119-128.
30. Gerlach, A.; Knebel, G.; Guber, A.E.; Heckele, M.; Herrmann, D.; Muslija, A.; and Schaller, T. (2002). "Microfabrication of single-use plastic microfluidic devices for high-throughput screening and DNA analysis." *Microsystem Technologies* (v7, n5-6), pp265-268.
31. Chien, F.S.; Hsieh, W.F.; Gwo, S.; Vladar, A.E.; and Dagata, J.A. (2002). "Silicon nanostructures fabricated by scanning probe oxidation and tetra-methyl ammonium hydroxide etching." *Journal of Applied Physics* (v91), pp10044.
32. Matsumoto, K.; Gotoh, Y.; Maeda, T.; Dagata, J.A.; and Harris, J. (2000). "Room-temperature single-electron memory made by pulse-mode atomic force microscopy nano oxidation process on atomically flat α-alumina substrate." *Applied Physics Letters* (v76, n2), pp239-241.
33. Dagata, J.A. (1995). "Device fabrication by scanned probe oxidation." *Science* (v270), pp1625-1626.
34. Dagata, J.A.; Schneir, J.; Harary, H.H.; Evans, C.J.; Postek, M.T.; and Bennett, J. (1990). "Modification of hydrogen-passivated silicon by a scanning tunneling microscope operating in air." *Applied Physics Letters* (v56), pp2001-2003.
35. Gale, M.T. (1997). "Replication." *Micro-optics, Elements, Systems, and Applications*, Herzig, H.P., ed. London: Taylor and Francis.
36. Halley, J.; Helvey, A.; Smith, K.S.; and Winfough, W.R. (1999). "The impact of high-speed machining on the design and fabrication of aircraft components." *Proc.* of 17th Biennial Conf. on Mechanical Vibration and Noise, 1999 ASME Design and Technical Conf., Sept. 12-16, 1999, Las Vegas, NV.
37. Smith, S.T. (2000). *Flexures*. London: Gordon and Breach Science Publishers.

Authors' Biographies

Tony L. Schmitz is an assistant professor in the Dept. of Mechanical and Aerospace Engineering at the University of Florida. He received his PhD in mechanical engineering from the University of Florida in 1999. He was then employed at the National Institute of Standards and Technology, first as an NRC postdoctoral research associate, then as a mechanical engineer from 1999 to 2002. His fundamental research area is precision manufacturing, which includes various projects in high-speed machining, optical metrology, and uncertainty analysis.

John A. Dagata is with the Precision Engineering Division of the National Institute of Standards and Technology (NIST). His research has involved the development and application of scanning probe methods and instrumentation for the fabrication and characterization of ultra-small structures. Prior appointments include a postdoctoral position at the Naval Research Laboratory (NRL) after receiving his PhD in physical chemistry from Louisiana State University, where he pioneered scanning probe oxidation as a resistless lithography technique. In 1996, he received the Department of Commerce (DoC) Bronze Award and in 2002 was awarded the DoC Gold Medal.

Brian Dutterer holds a shared appointment between the Manufacturing Metrology and Fabrication Technology Divisions at the National Institute of Standards and Technology. He has collaborated in the design and development of several specialized instruments using fabrication methods such as high-speed machining, diamond turning, and electrical discharge machining. He is also active is high-speed machining process dynamics research, particularly with application to the aerospace industry.

W. Gregory Sawyer is an assistant professor in the Dept. of Mechanical and Aerospace Engineering at the University of Florida. He received his PhD in mechanical engineering from Rensselaer Polytechnic Institute in 1999. He then joined the University of Florida faculty and established the Tribology Laboratory. His primary interests are in tribology, particularly solid-lubrication and sliding contacts in extreme environments, where the use of fluid lubrication is not available.